ARTHRITIS & RHEUMATISM
Vol. 63, No. 5, May 2011, pp 1246–1254
DOI 10.1002/art.30292

Rituximab Treatment Induces the Expression of Genes Involved in Healing Processes in the Rheumatoid Arthritis Synovium

I. Gutierrez-Roelens,[1] C. Galant,[1] I. Theate,[1] R. J. Lories,[2] P. Durez,[1] A. Nzeusseu-Toukap,[1] B. Van den Eynde,[3] F. A. Houssiau,[1] and B. R. Lauwerys[1]

Objective. **Rituximab displays therapeutic benefits in the treatment of patients with rheumatoid arthritis (RA) resistant to tumor necrosis factor (TNF) blockade. However, the precise role of B cells in the pathogenesis of RA is still unknown. We undertook this study to investigate the global molecular effects of rituximab in synovial biopsy samples obtained from anti-TNF–resistant RA patients before and after administration of the drug.**

Methods. **Paired synovial biopsy samples were obtained from the affected knee of anti-TNF–resistant RA patients before (time 0) and 12 weeks after (time 12) initiation of rituximab therapy. Total RNA was extracted, labeled according to standard Affymetrix procedures, and hybridized on GeneChip HGU133 Plus 2.0 slides. Immunohistochemistry and quantitative real-time reverse transcriptase–polymerase chain reaction experiments were performed to confirm the differential expression of selected transcripts.**

Results. **According to Student's paired *t*-tests, 549 of 54,675 investigated probe sets were differentially expressed between time 0 and time 12. Pathway analysis revealed that genes down-regulated between time 0 and time 12 were significantly enriched in immunoglobulin genes and genes involved in chemotaxis, leukocyte activation, and immune responses (Gene Ontology annotations). In contrast, genes up-regulated between time 0 and time 12 were significantly enriched in transcripts involved in cell development (Gene Ontology annotation) and wound healing (Gene Set Enrichment Analysis). At baseline, higher synovial expression of immunoglobulin genes was associated with response to therapy.**

Conclusion. **Rituximab displays unique effects on global gene expression profiles in the synovial tissue of RA patients. These observations open new perspectives in the understanding of the biologic effects of the drug and in the selection of patients likely to benefit from this therapy.**

Rituximab, originally developed for the treatment of B cell lymphoma, is a chimeric IgG1 monoclonal antibody directed against CD20, expressed on several subsets of B cells (1). It induces B cell depletion by complement- and antibody-mediated cytotoxicity (2). Therapeutic benefits of rituximab were reported in the treatment of several autoimmune diseases (idiopathic thrombocytopenic purpura, multiple sclerosis, and antineutrophil cytoplasmic antibody–associated vasculitis) (3–6). Recently, rituximab was also approved for the treatment of patients with refractory rheumatoid arthritis (RA) with inadequate responses to anti–tumor necrosis factor (anti-TNF) therapy (7–9). However, it is not fully understood how depletion of B cells interferes with RA pathogenesis.

To obtain a global molecular picture of the effects of rituximab on synovial tissue, we investigated

Supported by an unrestricted grant from Roche Belgium and by grants from the Fondation Saint-Luc (Cliniques Universitaires Saint-Luc), the Fonds de la Recherche Scientifique et Médicale (Belgium), and the Fonds Spécial de Recherche (Communauté française de Belgique). Dr. Gutierrez-Roelens is recipient of a fellowship from the Région Wallone (BioWin, the Health Cluster of Wallonia). Dr. Lories is recipient of a postdoctoral fellowship from the Flanders Research Foundation (FWO-Vlaanderen).

[1]I. Gutierrez-Roelens, PhD, C. Galant, MD, PhD, I. Theate, MD, P. Durez, MD, A. Nzeusseu-Toukap, MD, F. A. Houssiau, MD, PhD, B. R. Lauwerys, MD, PhD: Cliniques Universitaires Saint-Luc and Université catholique de Louvain, Brussels, Belgium; [2]R. J. Lories, MD, PhD: Katholieke Universiteit Leuven, Leuven, Belgium; [3]B. Van den Eynde, MD, PhD: Ludwig Institute for Cancer Research, Brussels Branch, and de Duve Institute, Brussels, Belgium.

Address correspondence to B. R. Lauwerys, MD, PhD, Department of Rheumatology (RUMA 5390), Cliniques Universitaires Saint-Luc, Avenue Hippocrate 10, B-1200 Brussels, Belgium. E-mail: Bernard.Lauwerys@uclouvain.be.

Submitted for publication May 30, 2010; accepted in revised form February 3, 2011.

transcriptomic profiles in synovial biopsy samples obtained from a prospective cohort of rituximab-treated, anti-TNF–resistant RA patients at baseline and 12 weeks after initiation of therapy. We have previously demonstrated that transcriptomic studies in synovial biopsy samples yield intelligible information (e.g., about specific molecular pathways involved in RA versus lupus arthritis or osteoarthritis) (10). Transcriptomic studies also enabled us to characterize molecular pathways affected by TNF blockade in the RA synovium. Thus, we found that adalimumab therapy induces a significant decrease in the synovial expression of genes involved in cell proliferation in RA. In the same study, we found that baseline synovial overexpression of genes induced by TNFα, interleukin-1β (IL-1β), and combinations of TNFα and IL-1β or TNFα and IL-17 is associated with poor response to adalimumab therapy, thereby indicating that these cytokines could play a role in the mechanisms of resistance to TNF blockade in RA (11).

In this study, we sought to determine whether distinct molecular pathways were associated with response to rituximab therapy in patients with severe RA. We found that rituximab induces a specific signature characterized by down-regulation of immunoglobulin and inflammatory genes and up-regulation of genes involved in healing processes.

PATIENTS AND METHODS

Patients and synovial biopsy samples. Twenty patients with RA (17 women and 3 men, mean ± SEM age 52.6 ± 3.8 years) were included in the study (Table 1). All patients met the American College of Rheumatology 1987 revised classification criteria for RA (12). All patients had active disease at the time of tissue sampling and were resistant to TNF blockade. They all had erosive changes imaged on conventional radiographs of the hands and/or feet. Each of them had a swollen knee at inclusion. Rituximab was administered intravenously (IV) at a dose of 1,000 mg at baseline (time 0) and at week 2, together with 125 mg IV methylprednisolone. Clinical parameters at baseline (time 0) and 12 weeks after the initiation of therapy (time 12) were evaluated with the Disease Activity Score in 28 joints (13) using the C-reactive protein level (DAS28-CRP), and clinical responses were assessed using the European League Against Rheumatism (EULAR) response criteria (14).

Synovial biopsy samples from all patients were obtained by needle arthroscopy of an affected knee at time 0 and time 12. For each procedure, 4–8 synovial samples were kept overnight at 4°C in an RNA stabilizing solution (RNALater; Ambion) and then stored at –80°C for later RNA extraction. The same amount of tissue was snap-frozen in liquid nitrogen and kept at –80°C for immunostaining experiments on frozen sections. The remaining material was fixed in 10% formaldehyde and embedded in paraffin for conventional optical evaluation and immunostaining of selected markers. All the experiments (RNA extraction, histology, immunohistochemistry) were performed on at least 4 biopsy samples harvested during every procedure in order to correct for variations related to the potential heterogeneous distribution of synovial inflammation. The study was approved by the ethics committee of the Université catholique de Louvain, and informed consent was obtained from all patients.

Table 1. Baseline characteristics of the 20 patients*

No. of women/no. of men	17/3
Age, mean ± SEM years	52.6 ± 3.8
Disease duration, mean ± SEM years	12.6 ± 1.9
DAS28-CRP, mean ± SEM	5.84 ± 0.28
CRP, mean ± SEM mg/liter	33.14 ± 5.94
No. with radiographic erosions	20
MTX therapy	
No. of patients	20
Dose, median (range) mg/week	15 (7.5–20)
Low-dose steroids	
No. of patients	15
Prednisolone dose, median (range) mg/day	5 (5–10)
No. of TNF-blocking agents used prior to rituximab therapy, median (range)	1 (1–3)
Washout period after discontinuation of TNF blockade, mean ± SEM months	2.5 ± 0.4

* DAS28-CRP = Disease Activity Score in 28 joints using the C-reactive protein level; MTX = methotrexate; TNF = tumor necrosis factor.

Microarray hybridization. Samples stored at –80°C after overnight incubation in RNALater were used for the microarray hybridizations. Total RNA was extracted from the synovial biopsy samples using the Nucleospin RNA II extraction kit (Macherey-Nagel), including DNase treatment of the samples. At least 1 μg total RNA could be extracted from 12 paired samples at time 0 and time 12 for further processing. RNA quality was assessed using an Agilent 2100 Bioanalyzer and RNA nanochips (Agilent).

Labeling of RNA (complementary RNA [cRNA] synthesis) was performed according to a standard Affymetrix procedure (One-Cycle Target Labeling kit; Affymetrix), as previously described (10). GeneChip HGU133 Plus 2.0 Arrays (spotted with 1,300,000 oligonucleotides, grouped in 54,675 probe sets informative for ~47,000 transcripts originated from not fewer than 39,000 genes; Affymetrix) were hybridized overnight at 45°C with 10 μg cRNA. The slides were then washed and stained using the EukGE-WS2v5 Fluidics protocol on the GeneChip Fluidics Station (Affymetrix) before being scanned on a GeneChip Scanner 3000. For the initial normalization and analysis steps, data were retrieved using Affymetrix GCOS software. The frequency of positive genes (genes with a flag present) was 40%–50% on each slide. After scaling of all probe sets to a value of 100, the range of the reported amplification scales was between 0.8 and 6.7. The signals yielded by the poly(A) RNA, hybridization, and housekeeping controls (GAPDH 3′:5′ probe sets signal intensities' ratio <2.3 in all the slides) were indicative of the good quality of the amplification and hybridization procedures. The Affymetrix .CEL and .CHP files were deposited in the GEO of the

National Center for Biotechnology Information and are accessible through GEO accession no. GSE24742.

Histopathology and immunohistochemistry analysis of paraffin-embedded sections. Fresh synovial biopsy tissue samples (n = 20 at time 0 and time 12) were fixed overnight in 10% formalin buffer at pH 7.0 and embedded in paraffin for histologic and immunohistochemical analyses. Serial histologic sections were stained with hematoxylin and eosin. The following parameters were evaluated: synovial hyperplasia, diffuse cellular infiltrates, lymphoid structures, fibrinoid necrosis, and vascular hyperplasia. A global semiquantitative score including the whole biopsy areas was given for these parameters (on a 0–3 scale, where 0 indicates absence and 3 indicates high level). A specific score was assigned for the hyperplasia of the synovial lining layer (0 indicates one or two cell layers, 1 indicates three or four cell layers, 2 indicates five or six cell layers, and 3 indicates at least seven cell layers).

Immunolabeling experiments were performed using a standard protocol, as previously described (10,11). The following antibodies were used: anti-CD3 (NeoMarkers), anti-CD20 (Biocare Medical), anti-CD68 (DakoCytomation), anti-CD138 (DakoCytomation), anti–Ki-67 (DakoCytomation), anti–mesenchyme homeobox 2 (Novus Biologicals), anti–laminin α4 (Proteintech Group), anti–bone morphogenetic protein receptor type IA (anti-BMPRIA; Abgent), anti–phospho-Smad3 (Rockland), and anti–Ig κ light chain (Thermo Scientific).

For the phospho-Smad1/5 (Cell Signaling Technology) staining, a different protocol was used, as described previously (15). In order to enhance the sensitivity of the phospho-Smad1/5 staining, the ABC peroxidase system (Vectastain Universal Elite ABC kit; Vector) was used, which is based on the formation of avidin and biotinylated horseradish peroxidase macromolecular complex.

Semiquantitative analyses of CD3, CD15, CD20, CD68, CD138, and Ki-67 markers were performed in a blinded manner by 2 independent evaluators (CG, IT) using a semiquantitative score on a scale of 0–3 (0 indicates absence and 3 indicates high level). The interobserver correlation was >82% for all analyses. Semiquantitative analysis of anti–Ig κ light chain antibody was performed by counting the number of positive stained cells in 6 areas/slide. The semiquantitative analysis was also performed in a blinded manner by 2 evaluators (IGR, BRL), and the interobserver correlation was >90%. Quantitative analysis of the anti–mesenchyme homeobox 2, anti–laminin α4, anti-BMPRIA, anti–phospho-Smad3, and anti–phospho-Smad1/5 antibody–immunostained sections was performed using ImageJ software (NIH Image; National Institutes of Health) according to the Digital Image Analysis process (16). Six digitalized images (400× magnification) were obtained for each slide by an operator (IGR) who was blinded to the identity of the samples. Each image included lining and sublining regions when possible. When the distribution of the staining was heterogeneous, the images were obtained in order to be representative of the globality of the slide. The surface staining and the surface of the nuclei were determined for each image, and the area of staining was then normalized by calculating the ratio of surface staining to nuclei staining.

Quantitative real-time reverse transcriptase–polymerase chain reaction (RT-PCR) experiments. RNA was extracted from samples frozen in liquid nitrogen and stored at –80°C. Before cDNA synthesis, RNA quality was verified using an Agilent 2100 Bioanalyzer and RNA nanochips. Complementary DNA was synthesized from a subset of RNA that originated from 8 samples at time 0 and from 7 samples at time 12 using RevertAid Moloney murine leukemia virus RT (Fermentas) and oligo(dT) primers. Quantitative RT-PCR was performed on a MyiQ single-color RT-PCR detection system (Bio-Rad) using SYBR Green detection mix. For each sample, 5 ng cDNA was loaded in triplicate with 1× SYBR Green Mix (Applied Biosystems) and 8.8 μM primers. The melting curves obtained after each PCR amplification confirmed the specificity of the SYBR Green assays. Relative expression of the target genes in the studied samples was obtained using the $\Delta\Delta C_t$ method, as previously described (10,11).

The following primers were used: for β-actin (GenBank accession no. NM_001101.3), 5′-GGCATCGTGATGGACTCCG-3′ (forward) and 5′-TCGCTGTCCACCTTCCAG-3′ (reverse); for *BMPRIA* (GenBank accession no. NM_004329), 5′-AATGAAGTTGATGTGCCCTTG-3′ (forward) and 5′-GCAATTGGTATTCTTCCACGA-3′ (reverse); for *LAMA4* (GenBank accession no. NM_001105206), 5′-TCCACCTCAGTTACACCCAAG-3′ (forward) and 5′-AACACCTCCAACAAACACAGG-3′ (reverse); for *MEOX2* (GenBank accession no. NM_005924), 5′-CTCACCAGACTGAGGCGATAC-3′ (forward) and 5′-TCCCTTTTTCACATTCACCAG-3′ (reverse); and for *CD24* (GenBank accession no. NM_013230), 5′-CTGCTGGCACTGCTCCTAC-3′ (forward) and 5′-GAAGACGTTTCTTGGCCTGA-3′ (reverse). The amplification constant of each pair of primers is between 1.95 and 2.05.

Immunoglobulin quantification. Serum total IgG was measured by nephelometry on a BNII nephelometer (Siemens Healthcare Diagnostics). IgG titers were measured at baseline in the 20 RA patients included in this study and in 5 additional rituximab-treated RA patients. Measurements were performed as part of the clinical followup of the patients; the results were retrieved from their medical records.

Statistical analysis. Statistical analyses of microarray data were performed using TMEV software, version 4.0 (http://www.tm4.org/mev/). Differences in gene expression between time 0 and time 12 were evaluated using Student's paired *t*-tests (using a target *P* value less than 0.01, without corrections for multiple comparisons) after processing of the scaled data for elimination of the genes with a flag absent in more than half of the samples and selection of the remaining 8,000 genes that displayed the widest interindividual variations. Additional statistical analyses (Student's *t*-tests at baseline comparing responders with nonresponders) were performed using GeneSpring software (Agilent). For each slide, scaled data were normalized to the 50th percentile value for each chip and to the median value for each gene. Pathway analyses were performed using DAVID (Database for Annotation, Visualization, and Integrated Discovery) (17,18), an application that interrogates functional annotation databases (Gene Ontology annotations, Kegg pathways, Biocarta, and InterPro) and finds overrepresented biologic themes within a group of genes (http://david.abcc.ncifcrf.gov/). The Gene Set Enrichment Analysis method was also used; this method compares gene expression profiles with gene sets previously reported in numerous experimental conditions (http://www.broadinstitute.org/gsea/index.jsp) (19).

RESULTS

Disease activity was prospectively evaluated in 20 anti-TNF–resistant RA patients at baseline (time 0) and 12 weeks after initiation of rituximab therapy (time 12) based on DAS28-CRP scores. All patients had active disease at baseline (mean ± SEM DAS28-CRP score 5.84 ± 0.28; mean ± SEM CRP level 33.14 ± 5.94 mg/liter). (The individual clinical, histologic, and immunohistochemical characteristics of the patients are shown in Supplementary Tables 1A–C, available on the *Arthritis & Rheumatism* Web site at http://onlinelibrary.wiley.com/journal/10.1002/(ISSN)1529-0131.) According to EULAR response criteria, 16 patients were considered responders (9 with a moderate response, 7 with a good response) and 4 were considered nonresponders (Figure 1). Rituximab induced a depletion of synovial CD20+ cells in 18 of 20 treated patients at time 12. Semiquantitative evaluation of CD68+ cells also showed a decrease between time 0 and time 12, although this was not significant. No correlations were found between changes in CD20+ or CD68+ cells and changes in the DAS28-CRP score or any of its components. The amounts of CD3+, CD15+, and CD138+ cells did not differ between time 0 and time 12.

The molecular effects of rituximab were investigated using high-density oligonucleotide-spotted microarrays. Enough total RNA (>1 μg) was extracted from 12 synovial biopsy samples at time 0 and time 12, labeled, and hybridized on GeneChip HGU133 Plus 2.0 Arrays according to standard Affymetrix procedures. According to Student's paired *t*-tests, 549 of 54,675 probe sets were differentially expressed between time 0 and time 12; 220 of them were up-regulated and 329 were down-regulated (see Supplementary Table 2, available on the *Arthritis & Rheumatism* Web site at http://onlinelibrary.wiley.com/journal/10.1002/(ISSN)1529-

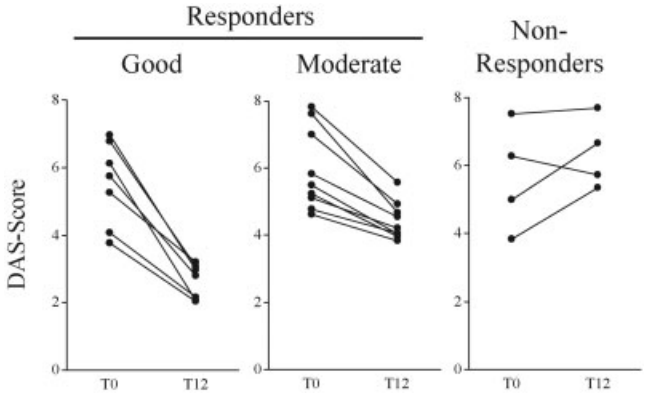

Figure 1. Evolution of Disease Activity Score (DAS) (4 variables) in 20 individual rheumatoid arthritis patients before (time 0 [T0]) and 12 weeks after (time 12 [T12]) initiation of rituximab therapy. Patients were categorized as responders (good or moderate) or nonresponders according to European League Against Rheumatism criteria.

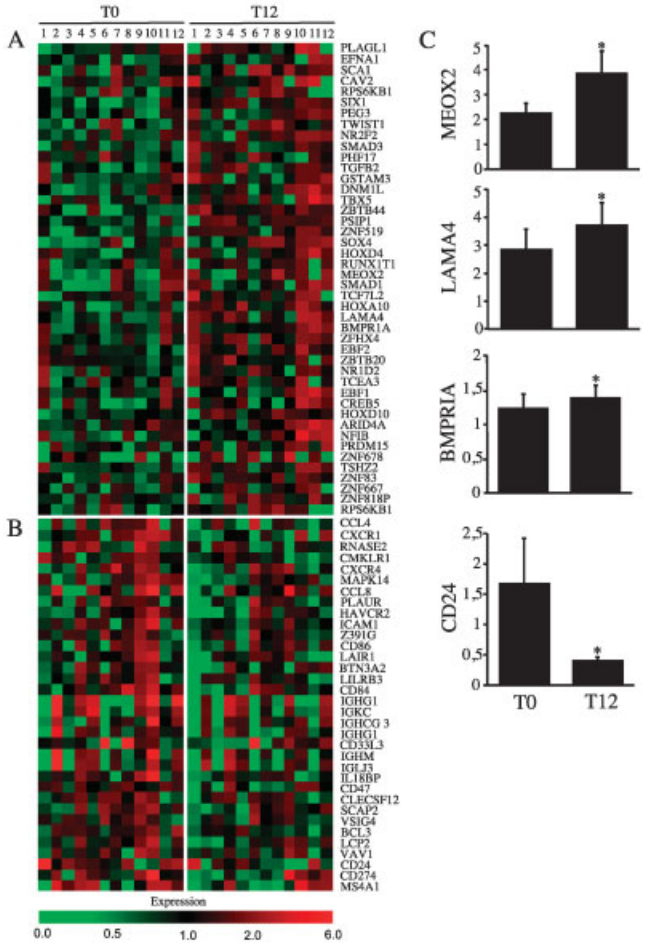

Figure 2. Genes differentially expressed before (time 0 [T0]) and 12 weeks after (time 12 [T12]) the start of rituximab therapy in synovial biopsy samples (numbered from 1 to 12) from rheumatoid arthritis patients. Student's paired *t*-tests indicated that 549 of 54,675 probe sets displayed significant differences in expression between time 0 and time 12. Pathway analyses indicated that a significant percentage of these genes clustered into distinct pathways. **A,** Up-regulated genes were significantly enriched in transcripts involved in developmental processes, cell development, and transforming growth factor β signaling. **B,** Down-regulated genes were significantly enriched in immunoglobulin genes and in transcripts involved in immune responses, chemotaxis, and leukocyte activation. **C,** Shown are results of real-time reverse transcriptase–polymerase chain reaction studies of the expression of selected genes in rheumatoid arthritis synovial biopsy tissue before (n = 8) and 12 weeks after (n = 7) initiation of rituximab therapy. Samples were loaded in triplicate. Results were normalized to β-actin and are the mean ± SEM gene expression, relative to the mean gene expression in a standard sample normalized to 1. * = $P < 0.05$ versus time 0.

0131). Not surprisingly, pathway analyses (Gene Ontology mining software and Gene Set Enrichment Analyses) indicated that genes down-regulated by rituximab were significantly enriched in immunoglobulin genes. Moreover, rituximab also induced a significant down-regulation of transcripts involved in immune responses, chemotaxis, and leukocyte activation (Gene Ontology annotation). In contrast, genes up-regulated by rituximab were significantly enriched in transcripts involved in cell development (Gene Ontology annotation), developmental processes (Gene Ontology annotation), transforming growth factor β (TGFβ) signaling (Gene Ontology annotation), and wound healing (Gene Set Enrichment Analyses) (Figures 2A and B). In order to confirm the microarray data, a few genes were randomly selected, with a particular focus on genes involved in developmental processes. The differential expression of these genes (*BMPRIA*, *LAMA4*, *MEOX2*, and *CD24*) was confirmed by real-time RT-PCR experiments (Figure 2C).

Many of the genes induced by rituximab and belonging to the cell development, developmental processes, or TGFβ signaling pathways (by Gene Ontology annotation) or to the wound healing pathway (by Gene Set Enrichment Analyses) are known to play a role in the differentiation of mesenchymal cell progenitors in the developing skeleton. In order to confirm the rituximab-induced effects on the up-regulation of these genes, we performed immunohistochemistry experiments on synovial biopsy samples from the 20 patients involved in the study. We evaluated synovial expression of BMPRIA (a bone morphogenetic protein receptor) and laminin α4 and mesenchyme homeobox 2 (markers of mesenchymal cell differentiation). Quantitative evaluation of the slides confirmed that these 3 molecules were significantly induced in synovial biopsy samples after rituximab therapy (Figures 3A and B).

Up-regulation of these genes prompted us to investigate whether administration of rituximab resulted in synovial activation of TGFβ or BMP signaling. To explore this hypothesis, we performed immunohistochemistry studies on phospho-Smad3 (a marker of TGFβ activation) and phospho-Smad1/5 (a marker of BMP activation). No significant difference in phospho-Smad3 staining was observed between time 0 and time 12. The phospho-Smad1/5 signal decreased significantly between time 0 and time 12 (Figures 3C and D). These results indicate that synovial up-regulation of genes involved in developmental processes is not associated with increased TGFβ or BMP activity through its canonical pathways at time 12.

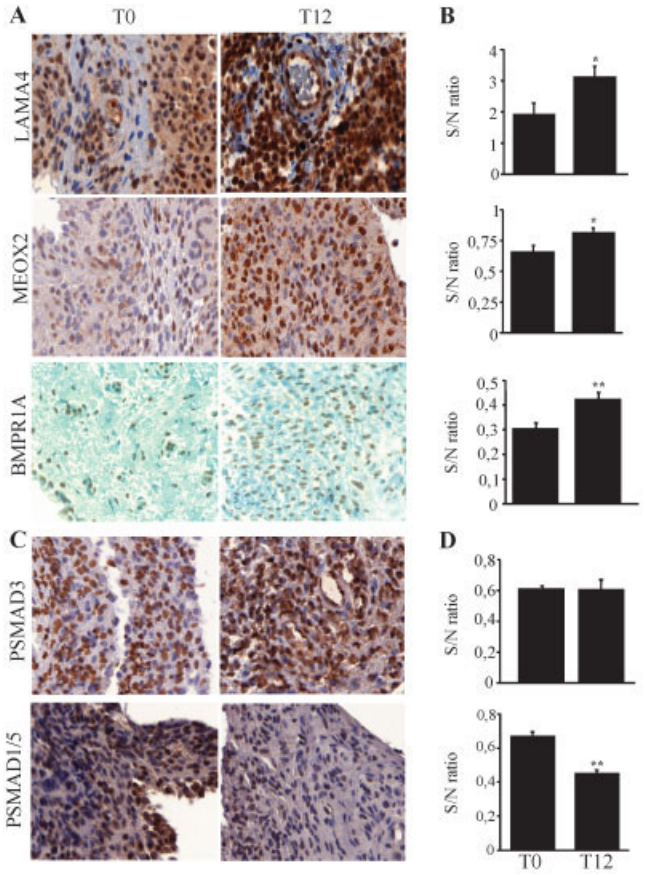

Figure 3. Changes in immunohistochemistry parameters in the synovial biopsy samples from rheumatoid arthritis patients, collected prior to (time 0 [T0]; n = 20) and 12 weeks after (time 12 [T12]; n = 20) initiation of rituximab therapy. **A** and **C,** Characteristic images of the stained markers laminin α4 (LAMA4), mesenchyme homeobox 2 (MEOX2), and bone morphogenetic protein receptor type IA (BMPRIA) (**A**) and phospho-Smad3 (PSMAD3) and phospho-Smad1/5 (PSMAD1/5) (**C**). Original magnification $\times$ 400. **B** and **D,** Ratio of surface staining to staining of the nuclei (S:N) for markers in **A** and **C**. Slides were analyzed using ImageJ software with 6 digitalized pictures (at 400$\times$ magnification) obtained for each sample. Results are the mean $\pm$ SEM. $* = P < 0.05$; $** = P < 0.005$ versus time 0, by Wilcoxon's matched pairs signed rank test.

Next, we investigated whether the molecular changes induced by rituximab in the synovium (in particular, the synovial up-regulation of genes involved in cell development and developmental processes) were a specific effect of rituximab or could be observed after administration of other drugs. We compared the differential expression of these genes in the paired synovial biopsy samples from our rituximab-treated RA patients with differential expression of the same genes observed between time 0 and time 12 in a previously described

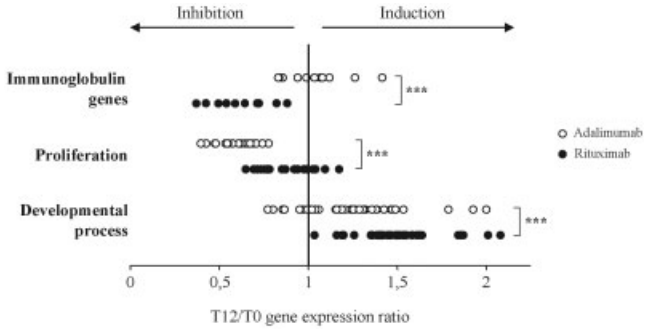

Figure 4. Comparison of the effects of rituximab and adalimumab on the expression of genes involved in specific pathways. The ratios of gene expression 12 weeks after initiation of rituximab or adalimumab therapy (time 12 [T12]) to expression before initiation of therapy (time 0 [T0]) were extracted from the microarray data for genes belonging to the Gene Ontology pathways of immunoglobulin genes, cell proliferation, and developmental processes (for gene lists and ratios, see Supplementary Table 5, available on the *Arthritis & Rheumatism* Web site at http://onlinelibrary.wiley.com/journal/10.1002/(ISSN)1529-0131). *** = $P < 0.0005$ by Student's *t*-test for paired values.

cohort of adalimumab-treated RA patients (11). We found that both drugs displayed distinct effects on global changes in gene expression. In particular, adalimumab displayed a significant inhibitory effect on the expression of genes involved in cell proliferation, while this was not the case with rituximab. In contrast, adalimumab had no effect on the expression of immunoglobulin genes. Both drugs induced the up-regulation of genes involved in developmental processes; however, the difference in gene expression was not significant with adalimumab, in contrast to the effect of rituximab (Figure 4) (see Supplementary Table 3, available on the *Arthritis & Rheumatism* Web site at http://onlinelibrary.wiley.com/journal/10.1002/(ISSN)1529-0131).

Interestingly, baseline expression of the genes involved in developmental processes was slightly although significantly lower in the biopsy samples from the rituximab-treated patients than in those from the adalimumab-treated patients. Moreover, we found a significantly lower negative correlation between baseline DAS28-CRP scores and baseline expression of these genes in the rituximab-treated group (the higher the baseline DAS28-CRP score, the lower the baseline expression of the genes) than in the adalimumab-treated group. Finally, induction of these genes correlated significantly more with the changes in DAS28-CRP scores between time 0 and time 12 in the rituximab-treated group (the higher the decrease in DAS28-CRP score, the higher the induction) than in the adalimumab-treated group (see Supplementary Table 3, available on the *Arthritis & Rheumatism* Web site at http://onlinelibrary.wiley.com/journal/10.1002/(ISSN)1529-0131). Taken together, these results are indicative of a significant imbalance between inflammation and repair in the synovial biopsy samples of the patients recruited in this study and treated with rituximab.

In a last set of analyses, we explored whether responders and nonresponders to rituximab therapy could be discriminated at baseline, based on clinical, histochemical, or molecular characteristics. We did not find any difference in baseline clinical (DAS28-CRP scores, CRP levels) and immunohistochemical (CD20+, CD3+, CD15+, CD68+, and CD138+ cells) parameters between responders and nonresponders. Of the 10 patients with serum rheumatoid factor positivity, 9 were either good or moderate responders, an enrichment that did not reach statistical significance in our population (see Supplementary Tables 1A–C, available on the *Arthritis & Rheumatism* Web site at http://onlinelibrary.wiley.com/journal/10.1002/(ISSN)1529-

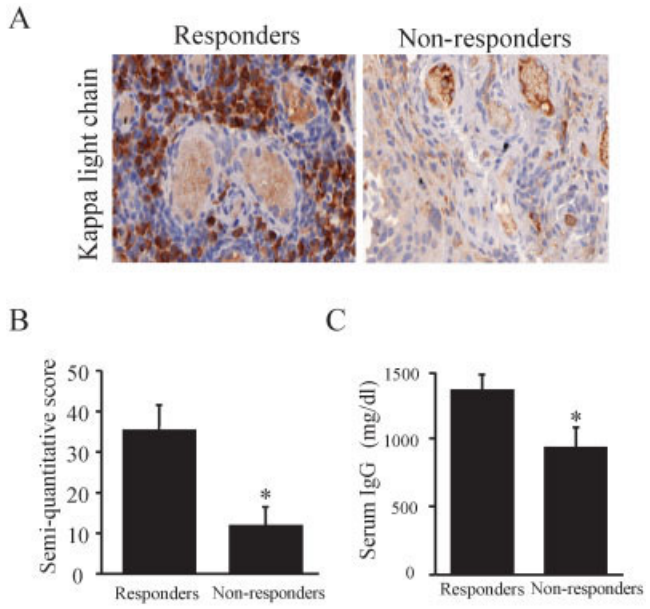

Figure 5. A, Baseline immunostaining for κ light chains in synovial biopsy samples from patients who responded (n = 17) and those who did not respond (n = 3) to rituximab therapy. Characteristic images are shown. Original magnification × 400. **B,** Semiquantitative analysis of the κ light chain immunostaining. Cells were counted in 6 areas/slide at 400× magnification. Results are the mean ± SEM number of cells from 6 areas. * = $P < 0.05$ versus responders, by Mann-Whitney U test. **C,** Baseline serum IgG levels in responders (n = 18) and nonresponders (n = 7) prior to rituximab therapy. Results are the mean ± SEM. * = $P < 0.05$ versus responders, by Mann-Whitney U test.

0131). In contrast, we found 2,458 genes to be differentially expressed in synovial biopsy samples from responders compared with nonresponders at baseline. Pathway analyses indicated that the genes up-regulated in responders were enriched in immunoglobulin genes and genes involved in antigen processing and presentation of antigen via class II major histocompatibility complex (MHC) molecules (see Supplementary Table 4, available on the *Arthritis & Rheumatism* Web site at http://onlinelibrary.wiley.com/journal/10.1002/(ISSN)1529-0131).

In order to confirm those results, we performed Ig κ light chain immunostaining experiments on the synovial biopsy samples at baseline. Semiquantification of the slides showed that baseline synovial biopsy samples from responders expressed significantly more Ig κ light chains than those from nonresponders (Figures 5A and B). In addition, baseline serum IgG levels were measured in 25 RA patients prior to initiation of rituximab therapy. Baseline serum IgG levels were significantly higher in responders than in nonresponders (Figure 5C).

DISCUSSION

We studied gene expression profiles in synovial biopsy samples from anti-TNF–resistant RA patients that were obtained prior to and 12 weeks after initiation of therapy. Genes down-regulated by rituximab therapy were immunoglobulin genes as well as genes involved in chemotaxis and leukocyte activation. Surprisingly, genes up-regulated by rituximab clustered in a very characteristic signature of cell development and wound healing. Real-time RT-PCR and immunohistochemistry experiments confirmed these observations at the messenger RNA and protein levels. At baseline, we also found that higher synovial expression of immunoglobulin light chains as well as higher IgG serum levels were associated with response to therapy.

The aim of our study was to obtain an overview of the pathways affected by rituximab in the RA synovium. Our access to paired synovial biopsy samples collected prospectively in a cohort of anti-TNF–resistant RA patients before and after rituximab therapy was a unique opportunity to investigate the effects of the drug on the site of chronic inflammatory processes characteristic of severe RA. Rituximab induced synovial B cell depletion in 18 of the 20 RA patients included, a rate in line with previous reports. In contrast, we did not observe any significant decrease in synovial macrophages, T cells, and plasma cells after rituximab therapy, as described in a previous report by Thurlings et al (20). The relatively small number of patients recruited in the present study, the use of semiquantitative rather than quantitative scores, and the fact that our patients had very severe disease (radiographic erosions, resistance to TNF blockade) are several factors that can explain this difference.

Global gene expression studies resulted in the unexpected observation that rituximab induces a very characteristic signature made of genes involved in cell development and wound healing in the synovium. Because the gene expression studies were performed using total synovial biopsy samples, it was important to rule out the possibility that this signature resulted from a proportional increase in followup biopsies of normal resident synovial cells and a proportional decrease in infiltrating inflammatory cells. In order to address this issue, we first compared the gene expression data generated in this study with data from previous work in which we had investigated the effects of adalimumab on cell populations and global gene expression profiles in RA synovial biopsy samples. In contrast to the effects of rituximab, adalimumab did induce a significant decrease in infiltrating cell populations in the synovium, particularly CD68+ cells in all patients treated, but also CD3+ and CD15+ cells in patients who responded to therapy. Despite the significant increase in resident synovial cells in the followup biopsy samples of the adalimumab study, the increased expression of genes involved in the TGFβ and cell differentiation signature was not of the same amplitude as that observed with rituximab, thereby suggesting that rituximab displays specific effects on the induction of these genes in the context of the present study.

Immunohistochemistry experiments further confirmed that rituximab displays significant effects on the induction of proteins involved in reparative processes in the synovium. In particular, we demonstrated that rituximab induced a significant up-regulation of BMPRIA, mesenchyme homeobox 2, and laminin α4 in followup biopsy samples. Bone morphogenetic protein receptors are cellular markers of mesenchymal progenitor cells. Their ligands are members of the TGFβ/BMP family of proteins, which play a pivotal role in the differentiation of mesenchymal-derived cells (particularly osteoblasts and chondrocytes), but also in reparative processes such as wound healing or callus formation. Similarly, mesenchyme homeobox 2 is expressed during later stages of embryonic limb and skeletal development and plays a role in the terminal differentiation of mesenchymal progenitor cells. Laminin α4 is also expressed in developing or regenerating tissues; it plays a particular role in

the formation of basal membranes and is therefore essential for the development of new blood vessels.

Rituximab and adalimumab display distinct effects on global gene expression profiles in the RA synovium. However, both drugs induced the expression of genes involved in reparative processes at time 12, thereby suggesting that increased expression of these genes is a common denominator associated with clinical improvement in RA synovitis. The relative difference in the induction of these genes observed between rituximab and adalimumab could be related to the fact that patients included in those 2 trials were at different stages of the disease. In favor of this hypothesis are 1) the significantly lower expression of genes involved in developmental processes in the baseline synovial samples from the rituximab-treated patients, 2) the significantly lower inverse correlation between baseline DAS28-CRP scores and baseline expression of these genes in the biopsy samples from the rituximab-treated patients (the higher the baseline DAS28-CRP score, the lower the baseline expression of the genes), and 3) the significantly higher correlation between changes in DAS28-CRP scores between time 0 and time 12 and induction of these genes observed in the rituximab-treated patients (the higher the decrease in the DAS28-CRP score, the higher the induction).

These observations support the hypothesis that the rituximab-treated patients were at a different stage of the disease, in which there is a significant imbalance between synovial inflammation and repair, thereby making them more susceptible to changes in expression of genes associated with healing processes during therapy. In addition, the differential effects of rituximab and adalimumab on the induction of genes involved in healing processes could also point to a potential role of B cells in the maintenance of pathogenic mechanisms in the RA synovium, associated with an inhibition of such reparative pathways. From this perspective, recent data obtained in a large cohort of RA patients were indicative of a significant inverse correlation between size and number of synovial B cell aggregates and expression of synovial BMP-2 and BMP-7, an observation that supports the presence of a link between B cells and inhibition of differentiation processes in the synovium (21).

The link between synovial B cell modulation and downstream activation of TGFβ/BMP signaling is still unclear. Looking at synovial patterns of Smad3 and Smad1/5 phosphorylation, we did not observe any sign of increased TGFβ or BMP signaling 12 weeks after administration of the drug. In contrast, we found that rituximab induced a significant decrease in synovial Smad1/5 phosphorylation, as previously observed in RA patients treated with TNF-blocking agents (15). The latter could be a secondary response, and compensatory mechanisms may be in place at this time point, effectively inhibiting the differentiation of mesenchymal cells toward cartilage or bone in the synovium itself. In contrast, activation of developmental cascades in the synovium may have a stimulatory effect on cartilage and bone in the vicinity of the joint, but further studies are required to substantiate this hypothesis.

Finally, we observed that higher baseline synovial immunoglobulin gene and protein expression were significantly associated with response to therapy. Further analyses indicated that baseline serum IgG levels were significantly higher in responders than in nonresponders. This observation is in line with previous reports indicating that the presence of serum rheumatoid factor is associated with response to rituximab therapy in RA (22,23). Although the overlap in baseline synovial and serum immunoglobulin concentrations did not enable adequate discrimination of responders and nonresponders on an individual basis, the difference might still be informative from a physiopathologic point of view. Gene expression data indicate that overexpression not only of immunoglobulin genes, but also of other genes involved in antigen presentation such as class II MHC molecules is associated with response to therapy. This might indicate that B cells in the synovium of RA patients display heterogeneous functional abilities, and that patients with synovial B cells actively involved in antigen presentation are more likely to respond to rituximab therapy. Further studies are needed to verify whether this observation can translate to the identification of clinically useful biomarkers, which will enable us to tailor the prescription of rituximab in RA according to the individual characteristics of the patients.

AUTHOR CONTRIBUTIONS

All authors were involved in drafting the article or revising it critically for important intellectual content, and all authors approved the final version to be published. Dr. Lauwerys had full access to all of the data in the study and takes responsibility for the integrity of the data and the accuracy of the data analysis.

Study conception and design. Gutierrez-Roelens, Galant, Theate, Lories, Durez, Nzeusseu-Toukap, Houssiau, Lauwerys.

Acquisition of data. Gutierrez-Roelens, Galant, Theate, Lories, Durez, Nzeusseu-Toukap, Houssiau, Lauwerys.

Analysis and interpretation of data. Gutierrez-Roelens, Galant, Theate, Lories, Durez, Van den Eynde, Houssiau, Lauwerys.

ROLE OF THE STUDY SPONSOR

Roche Belgium did not take part in the design of the study, collection or analysis of the data, or writing of the manuscript. The

manuscript was not previewed by Roche Belgium before submission, and publication was not contingent upon their approval.

REFERENCES

1. Coiffier B, Haioun C, Ketterer N, Engert A, Tilly H, Ma D, et al. Rituximab (anti-CD20 monoclonal antibody) for the treatment of patients with relapsing or refractory aggressive lymphoma: a multicenter phase II study. Blood 1998;92:1927–32.
2. Reff ME, Carner K, Chambers KS, Chinn PC, Leonard JE, Raab R, et al. Depletion of B cells in vivo by a chimeric mouse human monoclonal antibody to CD20. Blood 1994;83:435–45.
3. Godeau B, Porcher R, Fain O, Lefrere F, Fenaux P, Cheze S, et al. Rituximab efficacy and safety in adult splenectomy candidates with chronic immune thrombocytopenic purpura: results of a prospective multicenter phase 2 study. Blood 2008;112:999–1004.
4. Bar-Or A, Calabresi PA, Arnold D, Markowitz C, Shafer S, Kasper LH, et al. Rituximab in relapsing-remitting multiple sclerosis: a 72-week, open-label, phase I trial. Ann Neurol 2008;63:395–400.
5. Hauser SL, Waubant E, Arnold DL, Vollmer T, Antel J, Fox RJ, et al. B-cell depletion with rituximab in relapsing-remitting multiple sclerosis. N Engl J Med 2008;358:676–88.
6. Lovric S, Erdbruegger U, Kumpers P, Woywodt A, Koenecke C, Wedemeyer H, et al. Rituximab as rescue therapy in antineutrophil cytoplasmic antibody-associated vasculitis: a single-centre experience with 15 patients. Nephrol Dial Transplant 2009;24:179–85.
7. Emery P, Fleischmann R, Filipowicz-Sosnowska A, Schechtman J, Szczepanski L, Kavanaugh A, et al, for the DANCER Study Group. The efficacy and safety of rituximab in patients with active rheumatoid arthritis despite methotrexate treatment: results of a phase IIb randomized, double-blind, placebo-controlled, dose-ranging trial. Arthritis Rheum 2006;54:1390–400.
8. Cohen SB, Emery P, Greenwald MW, Dougados M, Furie RA, Genovese MC, et al, for the REFLEX Trial Group. Rituximab for rheumatoid arthritis refractory to anti–tumor necrosis factor therapy: results of a multicenter, randomized, double-blind, placebo-controlled, phase III trial evaluating primary efficacy and safety at twenty-four weeks. Arthritis Rheum 2006;54:2793–806.
9. Edwards JC, Leandro MJ, Cambridge G. B lymphocyte depletion therapy with rituximab in rheumatoid arthritis. Rheum Dis Clin North Am 2004;30:393–403, viii.
10. Nzeusseu Toukap A, Galant C, Theate I, Maudoux AL, Lories RJ, Houssiau FA, et al. Identification of distinct gene expression profiles in the synovium of patients with systemic lupus erythematosus. Arthritis Rheum 2007;56:1579–88.
11. Badot V, Galant C, Nzeusseu Toukap A, Theate I, Maudoux AL, Van den Eynde BJ, et al. Gene expression profiling in the synovium identifies a predictive signature of absence of response to adalimumab therapy in rheumatoid arthritis. Arthritis Res Ther 2009;11:R57.
12. Arnett FC, Edworthy SM, Bloch DA, McShane DJ, Fries JF, Cooper NS, et al. The American Rheumatism Association 1987 revised criteria for the classification of rheumatoid arthritis. Arthritis Rheum 1988;31:315–24.
13. Prevoo ML, van 't Hof MA, Kuper HH, van Leeuwen MA, van de Putte LB, van Riel PL. Modified disease activity scores that include twenty-eight–joint counts: development and validation in a prospective longitudinal study of patients with rheumatoid arthritis. Arthritis Rheum 1995;38:44–8.
14. Van Gestel AM, Prevoo ML, van 't Hof MA, van Rijswijk MH, van de Putte LB, van Riel PL. Development and validation of the European League Against Rheumatism response criteria for rheumatoid arthritis: comparison with the preliminary American College of Rheumatology and the World Health Organization/International League Against Rheumatism criteria. Arthritis Rheum 1996;39:34–40.
15. Verschueren PC, Lories RJ, Daans M, Theate I, Durez P, Westhovens R, et al. Detection, identification and in vivo treatment responsiveness of bone morphogenetic protein (BMP)-activated cell populations in the synovium of patients with rheumatoid arthritis. Ann Rheum Dis 2009;68:117–23.
16. Haringman JJ, Vinkenoog M, Gerlag DM, Smeets TJ, Zwinderman AH, Tak PP. Reliability of computerized image analysis for the evaluation of serial synovial biopsies in randomized controlled trials in rheumatoid arthritis. Arthritis Res Ther 2005;7:R862–7.
17. Dennis G Jr, Sherman BT, Hosack DA, Yang J, Gao W, Lane HC, et al. DAVID: Database for Annotation, Visualization, and Integrated Discovery. Genome Biol 2003;4:P3.
18. Huang DW, Sherman BT, Lempicki RA. Systematic and integrative analysis of large gene lists using DAVID bioinformatics resources. Nat Protoc 2009;4:44–57.
19. Subramanian A, Tamayo P, Mootha VK, Mukherjee S, Ebert BL, Gillette MA, et al. Gene set enrichment analysis: a knowledge-based approach for interpreting genome-wide expression profiles. Proc Natl Acad Sci U S A 2005;102:15545–50.
20. Thurlings RM, Vos K, Wijbrandts CA, Zwinderman AH, Gerlag DM, Tak PP. Synovial tissue response to rituximab: mechanism of action and identification of biomarkers of response. Ann Rheum Dis 2008;67:917–25.
21. Bugatti S, Manzo A, Vitolo B, Fusetti C, Caporali R, Pitzalis C, et al. Clinical, radiographic and biomolecular features of B cell synovitis in rheumatoid arthritis [abstract]. Arthritis Rheum 2010;62 Suppl:S260.
22. Quartuccio L, Fabris M, Salvin S, Atzeni F, Saracco M, Benucci M, et al. Rheumatoid factor positivity rather than anti-CCP positivity, a lower disability and a lower number of anti-TNF agents failed are associated with response to rituximab in rheumatoid arthritis. Rheumatology (Oxford) 2009;48:1557–9.
23. Tak PP, Rigby WF, Rubbert-Roth A, Peterfy CG, van Vollenhoven RF, Stohl W, et al, for the IMAGE Investigators. Inhibition of joint damage and improved clinical outcomes with rituximab plus methotrexate in early active rheumatoid arthritis: the IMAGE trial. Ann Rheum Dis 2011;70:39–46.